Resonance Raman Spectroscopy Reveals a_{1u} vs a_{2u} Character and Pseudo-Jahn-Teller Distortion in Radical Cations of Ni^{II}, Cu^{II}, and $ClFe^{III}$ Octaethyl- and Tetraphenylporphyrins

Roman S. Czernuszewicz,[†] Kathleen A. Macor,[†,‡] Xiao-Yuan Li,[†] James R. Kincaid,[§] and Thomas G. Spiro*,[†]

Contribution from the Departments of Chemistry, Princeton University, Princeton, New Jersey 08544, and Marquette University, Milwaukee, Wisconsin 53233.
Received August 1, 1988

Abstract: Resonance Raman (RR) spectra have been analyzed for porphyrin radical cations prepared electrochemically from the Ni^{2+}, Cu^{2+}, VO^{2+}, and $(Cl^-)Fe^{3+}$ complexes of octaethylporphyrin (OEP) and *meso*-tetraphenylporphyrin (TPP). Band assignments have been secured via polarization measurements and isotope frequency shifts associated with ^{15}N and *meso*-d_4 (OEP) or pyrrole-d_8 and phenyl-d_{20} (TPP) substitution. These isotope shifts are similar to those of the neutral metalloporphyrins, establishing that the normal mode compositions for high-frequency skeletal modes are not significantly altered by radical formation. There are, however, appreciable changes in the mode frequencies between neutral porphyrin and radical cation, which are different for the OEP's and TPP's. In particular, the mode ν_2, which is largely pyrrole $C_\beta C_\beta$ stretching in character, shifts up and down upon radical formation in OEP's and TPP's, respectively. These are the directions expected if the OEP and TPP radicals have a_{1u} and a_{2u} character, respectively, since the a_{1u} and a_{2u} orbitals are antibonding and bonding, respectively, with respect to the $C_\beta C_\beta$ bonds. The pyrrole half-ring stretch, ν_4, shifts down on OEP radical formation, consistent with the $C_\alpha C_\beta$ bonding character of the a_{1u} orbital. The a_{2u} orbital is slightly antibonding with respect to the $C_\alpha N$ and $C_\alpha C_\beta$ bonds, and the TPP radical ν_4 shifts are smaller and variable. A novel feature of the radical cation RR spectra is the appearance of anomalously polarized bands in the $\sim$1000-cm^{-1} region with excitation near the Soret electronic transitions. These bands are sensitive to *meso*-d_4 (OEP) or pyrrole-d_8 (TPP) substitution, but neither their frequencies nor their isotope shifts correlate with A_{2g} modes of the neutral porphyrins. These bands are suggested to reflect pseudo-Jahn-Teller mixing between the A_{1u} and A_{2u} electronic states via the A_{2g} vibrational modes ($A_{1u} \times A_{2u} = A_{2g}$). The resulting decrease in the A_{2g} force constants greatly lowers the frequencies and remixes the mode compositions. It is further suggested that the saddle distortion observed in several porphyrin radical cation crystal structures so far reported might also be a pseudo-Jahn-Teller manifestation. The normal mode associated with the saddle distortion is B_{2u} in D_{4h} symmetry, but A_2 in the D_{2d} symmetry induced by the saddle distortion itself. The dynamic and/or static pseudo-Jahn-Teller distortions can account for the A_{1u}/A_{2u} mixing which is evident from EPR spectra; they may also play a role in the electron-transfer dynamics of porphyrins and related aromatic macrocycles. Striking departures for the radical cations from the usual resonance enhancement pattern of metalloporphyrins (B-band resonant A_{2g} mode enhancement, Q- as well as B-band resonant A_{1g} mode domination) are discussed in terms of the altered electronic character of the excited states and their effects on A, B, and C term RR scattering mechanisms.

Porphyrin cation radicals are of considerable interest as the primary products of electron-transfer reactions in which porphyrins act as donors. In bacterial photoreaction centers, photoexcitation produces the radical cation of a bacteriochlorophyll special pair.[1] The dynamics of this process, and of porphyrin and chlorophyll electron-transfer processes generally, are under intensive study from both experimental[2] and theoretical[3] perspectives. The complex character of the electronic states of porphyrin and related aromatic macrocycles adds an interesting dimension to the problem. The two highest occupied molecular orbitals are of a_{1u} and a_{2u} symmetry in the idealized D_{4h} symmetry of the molecule, and are nearly degenerate. The symmetry properties of these orbitals and their energetics have been studied extensively.[4] Either one can lie higher in energy, depending on the nature of the peripheral substituents, of the central metal, and of its axial ligands, so that porphyrin radical cation can have a predominantly A_{1u} or A_{2u} ground state.

Resonance Raman (RR) spectroscopy provides a promising tool for studying molecular and electronic structure in porphyrin radicals. The frequencies of the RR bands are sensitive to changes in bonding and conformation, while their intensities are sensitive to the nature of the resonant electronic state(s). Several studies of porphyrin cation radical RR spectra have appeared,[5-8] but the results have been difficult to interpret. The vibrational frequency shifts upon radical formation have not appeared to agree with expectation based on radical type. In a previous study from this laboratory,[6] frequency shifts for metallooctaethylporphyrin (MOEP) radicals were found to differ in sign for M = Zn^{2+}, Mg^{2+}, and the Co^{3+} bromide adduct, on the one hand, and M = Ni^{2+}, Cu^{2+}, and the Co^{3+} perchlorate adduct on the other, suggesting a clear behavioral distinction between a_{1u} (former group) and a_{2u} radical types, but the shift directions were opposite to expectation from orbital symmetry arguments. Likewise Itoh and co-workers[5] thought the shift direction for some modes to be contrary to expectation for metallotetraphenylporphyrin (MTPP). Babcock and co-workers[7] discovered, however, that the reported a_{1u}-type $MOEP^{\bullet+}$ RR spectra were actually attributable to porphyrin diacid, which is produced as an impurity during radical preparation. RR scattering from the diacid is dominant even when it is a minor component because its strong Soret absorption band is much closer to the 406.7-nm laser wavelength which had been used for excitation[6] than are those of the radical cations. We have

[†] Princeton University.
[‡] Present address: Department of Chemistry, University of Notre Dame, Notre Dame, IN 46556.
[§] Marquette University.
* Author to whom correspondence should be addressed.

(1) Parson, W. W.; Ke, B. In *Photosynthesis: Energy Conversion by Plants and Bacteria*; Govindijee, Ed.; Academic Press: New York, 1983.
(2) (a) Wasielewski, M. R.; Niemczyk, M. P.; Svec, W. A.; Pewitt, E. B. *J. Am. Chem. Soc.* **1985**, *107*, 1080-1082. (b) Ho, P. S.; Sutoris, C.; Liang, N.; Margoliash, E.; Hoffman, B. M. *J. Am. Chem. Soc.* **1985**, *107*, 1070-1071.
(3) (a) Jortner, J. *Biochim. Biophys. Acta* **1980**, *594*, 193-230. (b) Marcus, R. A.; Sutin, N. *Biochim. Biophys. Acta* **1985**, *811*, 265-322.
(4) (a) Gouterman, M. In *The Porphyrins*; Dolphin, D., Ed.; Academic Press: New York, 1978; Vol. III. (b) Spellane, P. J.; Gouterman, M.; Antepas, A.; Kim, S.; Liu, Y. C. *Inorg. Chem.* **1980**, *19*, 386-391.
(5) Yamaguchi, H.; Nakano, M.; Itoh, K. *Chem. Lett.* **1982**, 1397-1400.
(6) Kim, D.; Miller, L. A.; Rakhit, G.; Spiro, T. G. *J. Phys. Chem.* **1986**, *90*, 3320-3325.
(7) Salehi, A.; Oertling, W. A.; Babcock, G. T.; Chang, C. K. *J. Am. Chem. Soc.* **1986**, *108*, 5630-5631.
(8) Oertling, W. A.; Salehi, A.; Chung, Y. C.; Leroi, G. E.; Chang, C. K.; Babcock, G. T. *J. Phys. Chem.* **1987**, *91*, 5887-5898.

0002-7863/89/1511-3860$01.50/0

since confirmed that the spectra previously ascribed to OEP radicals of Zn^{2+}, Mg^{2+}, and Co^{3+} bromide are due to H_4OEP^{2+}. In a subsequent paper Oertling et al.[8] obtained authentic RR spectra for these $MOEP^{\bullet+}$ species and found that they all give the same pattern of frequency shifts as do $NiOEP^{\bullet+}$, $CuOEP^{\bullet+}$, and $[CoOEP^{\bullet+}](ClO_4)_2$. They concluded from this observation that similar shifts are induced by radical formation, regardless of the symmetry type.

In the present study we reinvestigate the RR spectra of porphyrin radical cations, this time for TPP (tetraphenylporphyrin) as well as OEP using the Ni^{2+}, Cu^{2+}, VO^{2+}, and $ClFe^{3+}$ complexes. We now have the benefit of detailed normal mode assignments for NiTPP[9] as well as NiOEP.[10] In the present work the radical cation RR spectra are analyzed in the light of these assignments using isotope shifts to label the modes. The frequency shifts upon radical formation differ for OEP and TPP; in particular, the A_{1g} mode ν_2, which is primarily $C_\beta C_\beta$ stretching in character, shifts up for the OEP but down for the TPP complexes. These shift directions make sense if the TPP radicals have a_{2u} character, as generally accepted,[11] but the OEP radicals all have a_{1u} character. We believe that the OEP radicals do have predominantly a_{1u} character, consistent with EPR analyses of the Mg^{2+} and Zn^{2+} complexes.[12] The attribution of a_{2u} to some OEP radicals, notably Ni^{2+}, Cu^{2+}, and the Co^{3+} perchlorate adduct, was based on differences in optical absorption spectra.[13] As argued below these are unlikely to be reliable indicators of radical type.

Although a_{1u} and a_{2u} may be good approximate designations for radical character, it is known from the EPR results[14] and ab initio calculations[15] that these states are not pure, since spin density appears on atoms which should occupy nodal positions on the basis of orbital symmetry. The RR spectra strongly suggest that an important mechanism for a_{1u}/a_{2u} mixing is the pseudo-Jahn–Teller (pJT) effect, in which the two states are mixed by a distortion along suitable vibrational modes, in this case the A_{2g} modes, since $A_{1u} \times A_{2u} = A_{2g}$. The A_{2g} modes give rise to RR bands with anomalous polarization (ap), and for both OEP and TPP, the RR spectra show ap bands which are sensitive to ring deuteration, and are at much lower frequencies than the deuterium-sensitive ap bands of the neutral porphyrins. The frequency lowering is a natural consequence of the pJT mixing.

Finally, we note that the saddle distortion seen in four of the porphyrin cation radical structures so far reported[16-21] might also result from a pJT effect. The mode leading to this distortion, B_{2u} in D_{4h} symmetry, becomes A_2 in D_{2d} symmetry, which is induced by the saddle distortion itself, and is then able to mix the A_{1u} and A_{2u} states (B_1 and B_2 in D_{2d} symmetry). Static as well as dynamic pJT distortions might play a role in the dynamics of electron transfer from porphyrins and back to the radical cations.

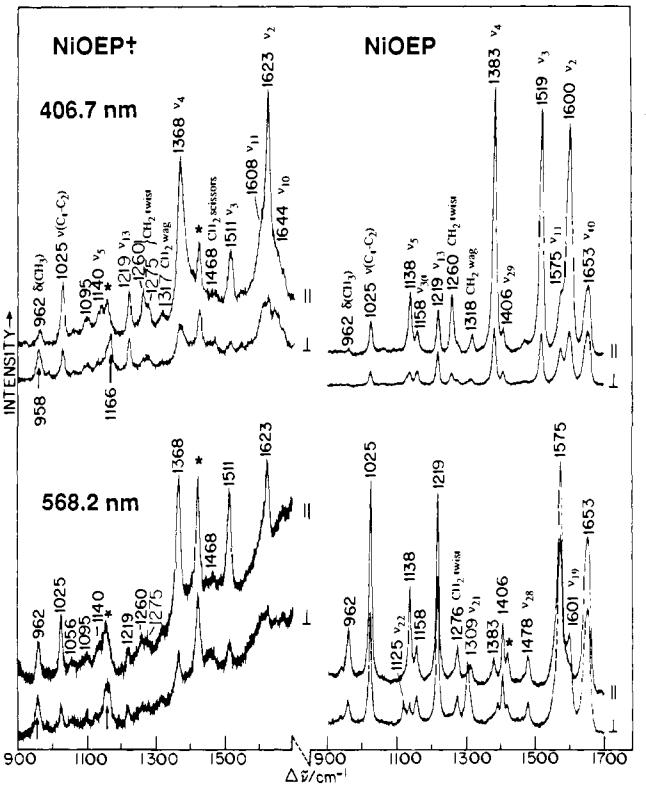

Figure 1. Resonance Raman spectra of NiOEP and $NiOEP^{\bullet+}$ in parallel (∥) and perpendicular (⊥) polarizations obtained with 406.7- and 568.2-nm excitation wavelengths. Spectra were obtained with 50-mW laser power and 8-cm^{-1} slitwidths. Asterisks indicate CH_2Cl_2 solvent bands.

Experimental Section

Chemicals. Metallooctaethyl- and metallotetraphenylporphyrins were obtained from Mid-Century Chemicals (Posen, IL) and in some cases purified on thin-layer alumina plates. Tetrabutylammonium perchlorate (TBAP) (GFS Chemicals, Columbus, OH) was recrystallized from ethyl acetate and dried under vacuum. Tetrabutylammonium tetrafluoroborate (TBAT) (Fluka Chemicals) was used as received. CH_2Cl_2 was distilled from CaH_2 prior to each use.

Electrochemical Oxidations and Raman Measurements. Bulk electrolyses were carried out at controlled potentials in a three-electrode glass Raman spectroelectrochemical cell similar in design to the low-temperature cell described recently by Czernuszewicz and Macor[22] with a Princeton Applied Research Model 173 potentiostat, Model 175 Universal programmer, and Model 179 Digital coulometer. The cell design allowed in situ Raman measurements in backscattering geometry.

Controlled-potential electrolyses were performed in dry CH_2Cl_2 containing 0.1 M TBAP or 0.1 M TBAT as supporting electrolyte. Spectra of NiOEP and its isotopically labeled complexes were also obtained in CD_2Cl_2 containing 0.1 M electrolyte. The course of electrooxidation was followed by continuously monitoring the ν_2 band region since the position of ν_2 is sensitive to porphyrin ring oxidation. Following oxidation and cation radical Raman data acquisition, the solutions were reduced at 0.2 V. In every case the characteristic neutral species spectrum was recovered.

Exciting radiation for RR measurements was produced by a Spectra Physics 171 Kr^+ laser (406.7, 568.2 nm) and a Spectra Physics Model 2025 Ar^+ laser (363.8, 457.9 nm). The scattered radiation was dispersed by a Spex 1401 monochromator and detected by a cooled RCA 31034A photomultiplier tube using an Ortec 9315 photon-counting system, under the control of a MINC II (DEC) minicomputer.

Results

1. Similar Radical RR Spectra with Violet and Yellow Excitation. Figure 1 compares RR spectra of NiOEP and its radical cation obtained with 406.7- and 568.2-nm excitation, while Figure 2 shows the positions of these laser lines in relation to the ab-

(9) Li, X.-Y.; Czernuszewicz, R. S.; Kincaid, J. R.; Spiro, T. G. *J. Phys. Chem.* **1989**, in press.
(10) Li, X.-Y.; Czernuszewicz, R. S.; Kincaid, J. R.; Stein, P.; Spiro, T. G. *J. Phys. Chem.* **1989**, in press.
(11) Fajer, J.; Borg, D. C.; Forman, A.; Dolphin, D.; Felton, R. H. *J. Am. Chem. Soc.* **1970**, *92*, 3451–3459.
(12) Fajer, J.; Borg, D. C.; Forman, A.; Felton, R. H.; Vegh, L.; Dolphin, D. *Ann. NY Acad. Sci.* **1973**, *206*, 349–364.
(13) Dolphin, D.; Muljiani, Z.; Rousseau, K.; Borg, D. C.; Fajer, J.; Felton, R. H. *Ann. NY Acad. Sci.* **1973**, *206*, 177–199.
(14) Fujita, E.; Chang, C. K.; Fajer, J. *J. Am. Chem. Soc.* **1985**, *107*, 7665–7669.
(15) Kashiwagi, H.; Obara, S. *Int. J. Quantum Chem.* **1981**, *20*, 843–859.
(16) Spaulding, L. D.; Eller, P. G.; Bertrand, J. A.; Felton, R. H. *J. Am. Chem. Soc.* **1974**, *96*, 982–987.
(17) Scholz, W. F.; Reed, C. A.; Lee, Y. J.; Scheidt, W. R.; Lang, G. *J. Am. Chem. Soc.* **1982**, *104*, 6791–6793.
(18) Buisson, G.; Deronzier, A.; Dûee, E.; Gans, P.; Marchon, J. C.; Regnard, J. R. *J. Am. Chem. Soc.* **1982**, *104*, 6793–6796.
(19) Barkigia, K. M.; Spaulding, L. D.; Fajer, J. *Inorg. Chem.* **1983**, *22*, 349–351.
(20) Gans, P.; Buisson, G.; Dûee, E.; Marchon, J. C.; Erler, B. S.; Scholz, W. F.; Reed, C. A. *J. Am. Chem. Soc.* **1986**, *108*, 1223–1234.
(21) (a) Spreer, L. O.; Maliyackel, A. C.; Holbrook, S.; Otvos, J. W.; Calvin, M. *J. Am. Chem. Soc.* **1986**, *108*, 1949–1953. (b) Scheidt, W. R.; Song, H.; Reed, C. A. *Abstracts of Papers*, 196th National Meeting of the American Chemical Society; American Chemical Society: Washington, DC, 1988; Abstract 144.
(22) Czernuszewicz, R. S.; Macor, K. A. *J. Raman Spectrosc.* **1988**, *19*, 553–557.

Table I. Resonance Raman Frequencies and ^{15}N Isotope Shifts (cm^{-1}) for NiOEP and $NiOEP^{\bullet+}$ and Their *meso*-d_4 Isotopomer[a]

	NiOEP				$NiOEP^{\bullet+}$				
ρ	NA	$\Delta^{15}N$	meso-d_4	$\Delta^{15}N$	NA	$\Delta^{15}N$	meso-d_4	$\Delta^{15}N$	assignment[b]
dp	1653	0	1642	0	1644	1	1638	0	ν_{10}, $\nu(C_\alpha-C_m)_{asym}$
p	1600	0	1599	0	1623	0	1621	0	ν_2, $\nu(C_\beta-C_\beta)$
dp	1575	0	1573	0	1608	0	1608	0	ν_{11}, $\nu(C_\beta-C_\beta)$
p	1519	1	1511	0	1511	3	1503	3	ν_3, $\nu(C_\alpha-C_\beta)_{sym}$
dp	1406	0	1406	0					ν_{29}, ν(pyr. quarter ring)
p	1383	7	1382	7	1368	10	1368	10	ν_4, ν(pyr. half ring)$_{sym}$
ap							1331	0	A_{2g} mode[c]
dp			1327	6					ν_{12}, ν(pyr. half ring)$_{sym}$
p	1318	0	1318	0	1317	0	1317	0	A_1, CH_2 wag
dp	1276	0			1275	0			B_1, CH_2 twist
p	1260	0	1259	0	1259	0	1259	0	A_1, CH_2 twist
dp	1219	1	948	10	1219	1	~950[d]	11	ν_{13}, $\delta(C_m-H)$
ap					1166	2	959	1	A_{2g} mode[c]
dp	1158	8	1158	9					ν_{30}, ν(pyr. half ring)$_{asym}$
p	1138	6	1138	6	1140	5	1140	6	ν_5, $\nu(C_\beta-C_1)_{sym}$
dp	1131	12	1186	2	1130	9	1181	1	ν_{14}, $\nu(C_\beta-C_1)_{sym}$
dp	1091	10	1090	8	1095	14			unassigned
p	1025[d]	2	1025	3	1025[d]	2	1026	2	A_1, $\nu(C_1-C_2)$
dp	1025[d]	2	1031	0	1025[d]	2	1033	0	B_1, $\nu(C_1-C_2)$
ap							989	1	A_{2g} mode[c]
p	962	2	963	3	962	3	960	3	$\delta(CH_3)$
ap					958	7	908	9	A_{2g} mode[c]

[a] Observed values in CH_2Cl_2/0.1 M TBAP solution spectra (406.7-nm excitation). NA = natural abundance; meso-d_4 = ^2H-substituted analogues at meso carbon positions; $\Delta^{15}N$ = frequency downshifts (cm^{-1}) upon pyrrole ^{15}N substitution; p, dp, and ap = polarized, depolarized, and anomalously polarized bands, respectively. [b] See ref 10 and 26 for mode descriptions. [c] New bands seen only in radical cation spectra. [d] Overlapping bands.[10]

sorption spectra of these species. The 406.7-nm line is close to resonance with the NiOEP B (Soret) absorption band. A-term scattering[23] is responsible for the strongest 406.7-nm excited bands, which are associated with totally symmetric modes and are polarized. The most intense bands (largest origin shifts) arise from the high-frequency skeletal modes ν_2, ν_3, and ν_4.[24] Depolarized bands (e.g., ν_{10}, ν_{11}, ν_{14}) are also seen with appreciable intensity, due to Jahn–Teller effects[25] associated with the B_{1g} coordinates. The 568.2-nm line is near resonance with the Q_0 absorption band, for which B-term activity[23] is dominant, and the vibronic mixing modes, B_{1g} and B_{2g} (depolarized, dp) and A_{2g} (anomalously polarized, ap), are strongly enhanced. Some A-term activity can still be seen, e.g., in the moderately strong polarized band at 1138 cm^{-1} (ν_5), but the bands which are strongest in the 406.7-nm excited spectrum are very weak at 568.2 nm.

The spectra of the radical cation are much weaker than those given by the neutral porphyrin, as can be gauged from the strength of the solvent bands at 1422 and 1156 cm^{-1}. Nevertheless, the contribution of residual neutral porphyrin to the radical cation spectra is very small, as can be seen from the negligible intensity remaining at the position of the strong bands at 1600 cm^{-1} in the 406.7-nm excited spectrum and at 1575 cm^{-1} in the 568.2-nm excited spectrum. Thus, conversion to the radical cation is very clean, thanks to the efficiency of the electrochemical cell. In contrast to NiOEP, $NiOEP^{\bullet+}$ gives similar RR spectra with 406.7- and 568.2-nm excitation. Spectra at both wavelengths are dominated by polarized modes, especially the three seen at 1623, 1511, and 1368 cm^{-1}. Depolarized bands can also be seen weakly. This result for 568.2-nm excitation supercedes the report by Kim et al.[6] that Q-band excited RR spectra are essentially the same for OEP radical cations as for the parent porphyrins. These earlier spectra, obtained at 77 K, were probably artifacts of photoreduction to the parent porphyrins in the stationary solid sample. In the present spectra the relative intensities differ somewhat at the two excitation wavelengths, but the enhancement pattern is remarkably similar and resembles that of the neutral porphyrin with 406.7-nm excitation. Thus the shape of the excited-state potential is similar for $NiOEP^{\bullet+}$, in both the violet and yellow regions, to that of NiOEP in the violet (B band). Oertling et al.[8] likewise report that RR spectra of $[Co^{III}OEP^{\bullet+}](Br^-)_2$ are dominated by polarized bands with red, as well as violet excitation. We observed the same pattern for $NiOEP^{\bullet+}$, $CuOEP^{\bullet+}$, $(VO)OEP^{\bullet+}$, and $(Cl^-)FeOEP^{\bullet+}$.

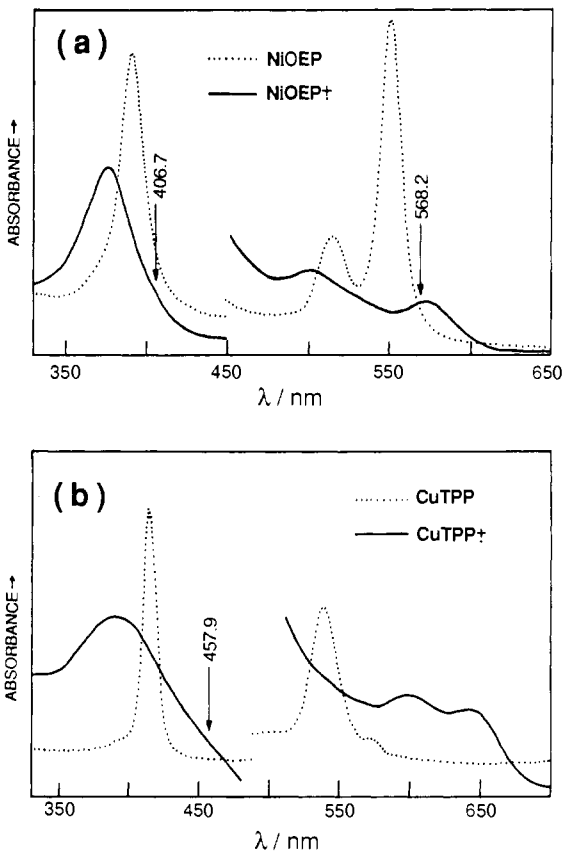

Figure 2. Absorption spectra of (a) NiOEP (···) and $NiOEP^{\bullet+}$ (—) and (b) CuTPP (···) and $CuTPP^{\bullet+}$ (—). The $MP^{\bullet+}$s were generated by electrooxidation in 0.1 M TBAP/CH_2Cl_2 in a thin-layer spectroelectrochemical cell. Absorbance rate for $MP^{\bullet+}$/MP is ~0.10. Arrows indicate excitation wavelengths used for Raman experiments.

(23) Spiro, T. G.; Li, X-Y. In *Biological Applications of Raman Spectroscopy*; Spiro, T. G., Ed.; Wiley-Interscience: New York, 1988; Vol. III, Chapter 1.

(24) Abe, M.; Kitagawa, T.; Kyogoku, Y. *J. Chem. Phys.* **1978**, *69*, 4526–4534.

(25) Shelnutt, J. A.; Cheung, L. D.; Cheng, C. C.; Yu, N. T.; Felton, R. H. *J. Chem. Phys.* **1977**, *66*, 3387–3398.

Table II. Resonance Raman Frequencies (cm^{-1}) for CuTPP and $CuTPP^{\bullet+}$ and Their Pyrrole-d_8 and Phenyl-d_{20} Isotopomers[a]

	CuTPP			$CuTPP^{\bullet+}$			
ρ	NA	d_8	d_{20}	NA	d_8	d_{20}	assignment[b]
p	1599	1600	1561	1595	1595	1561	ν(phenyl)
dp	1582[c]	1580[c]	1578[c]	1586	1586	1582	ν_{10}, $\nu(C_\alpha-C_m)_{asym}$
p	1562	1543	1568	1530	1508	1532	ν_2, $\nu(C_\beta-C_\beta)$
ap	1525[c]	1525[c]	1528[c]				ν_{19}, $\nu(C_\alpha-C_m)_{asym}$
dp	1501	1454	1501	1496	1453[d]	1501	ν_{11}, $\nu(C_\beta-C_\beta)$
dp				1452	1453[d]	1458	ν_{28}, $\nu(C_\alpha-C_m)_{sym}$
dp				1360	1326	1350[d]	ν_{29}, ν(pyr. quarter ring)
p	1365	1356	1360	1355	1351	1346	ν_4, ν(pyr. half ring)$_{sym}$
p	1237	1235	1186	1234	1235	1189	ν_1, $\nu(C_m-Ph)$
dp				1181	1183	863	$\delta(C_{Ph}-H)$
p	1080		1080	1077		1080	ν_9, $\delta(C_\beta-H)_{sym}$
ap				1044	950	1052	A_{2g} mode[e]
p	1008	1002	997	1002	1003	995	ν_6, ν(pyr. breathing)
p				990	983	990[d]	unassigned
ap				959	971	964	A_{2g} mode[e]
p	908	909	910	907	908	907	unassigned
ap				899	1023	903	A_{2g} mode[e]
p	886	891	889	884	888	891	ν_7, δ(pyr. def.)$_{sym}$

[a] Observed frequencies in CH_2Cl_2/0.1 M TBAP solution spectra (457.9 nm excitation). NA = natural abundance; d_8 and d_{20} = ^2H substituted analogues at pyrrole C_β and phenyl carbon positions, respectively; p, dp, and ap = polarized, depolarized, and anomalously polarized bands, respectively. [b] See ref 9 for mode descriptions. [c] Seen with 530.9-nm excitation. [d] Overlapping bands.[9] [e] New bands seen only in radical cation spectra.

Table III. Resonance Raman Frequencies (cm^{-1}) for Metallooctaethylporphyrins and Their Cation Radicals[a]

ρ	NiOEP	$NiOEP^{\bullet+}$	Δ	CuOEP	$CuOEP^{\bullet+}$	Δ	ClFeOEP	$ClFeOEP^{\bullet+}$	Δ	(OV)OEP	$(OV)OEP^{\bullet+}$	Δ	assignment[b]
dp	1653	1642	−9	1637	1632	−5	1628	1624	−4	1628	1621	−7	ν_{10}, $\nu(C_\alpha-C_m)_{asym}$
p	1600	1623	+23	1592	1613	+21	1579	1602	+23	1580	1601	+21	ν_2, $\nu(C_\beta-C_\beta)$
dp	1575	1608	+33	1568	1601	+33	1557			1558			ν_{11}, $\nu(C_\beta-C_\beta)$
p	1519	1511	−8	1503	1498	−4	1492	1490	−2	1494			ν_3, $\nu(C_\beta-C_\beta)_{sym}$
dp	1406			1406						1402			ν_{29}, ν(pyr. quarter ring)
p	1383	1368	−5	1378	1363	−15	1374	1362	−12	1376	1359	−17	ν_4, ν(pyr. half ring)$_{sym}$
ap		1331											A_{2g} mode[c]
p	1318	1317	−1	1320	1320	0	1322	1316	−6	1316	1306	−10	A_1, CH_2 wag
dp	1276	1275	−1	1274	1274	0	1272	1269	−3		1283		B_1, CH_2 twist
p	1260	1259	−1	1258	1259	+1	1257	1259	+2	1256	1255	−1	A_1, CH_2 twist
dp	1219	1219	0	1213	1216	+3	1209	1213	+4	1212	1212	0	ν_{13}, $\delta(C_m-H)$
ap		1166			1156						1149		A_{2g} mode[c]
dp	1158			1160			1155			1153			ν_{30}, ν(pyr. half ring)$_{asym}$
p	1138	1140	+2	1136	1136	0	1136	1140	+4	1135	1133	−2	ν_5, $\nu(C_\beta-C_1)_{sym}$
dp	1131	1130	−1		1132			1127			1121		ν_{14}, $\nu(C_\beta-C_1)_{sym}$
dp	1091	1095	+4		1098			1092			1091		unassigned
p, dp	1025[d]	1025[d]	0	1023[d]	1024[d]	+1	1025[d]	1026[d]	+1	1024[d]	1024[d]	0	A_1, B_1, $\nu(C_1-C_2)$
ap		958			938						931		A_{2g} mode[c]

[a] Observed frequencies in CH_2Cl_2/0.1 M TBAP solution spectra (406.7-nm excitation). Δ = frequency shifts (cm^{-1}) upon cation radical formation; p, dp, and ap = polarized, depolarized, and anomalously polarized bands, respectively. [b] See ref 10 and 26 for mode descriptions. [c] New bands seen only in radical cation spectra. [d] Overlapping bands.[10]

2. Isotope Shifts Show Normal Mode Constancy upon Radical Formation. The implication from the RR spectral similarities between NiOEP and $NiOEP^{\bullet+}$ is that the porphyrin normal mode compositions do not change greatly upon radical cation formation. This inference was directly confirmed via isotopic substitution. Figure 3 compares 406.7-nm excited spectra for isotopic species of NiOEP and $NiOEP^{\bullet+}$, involving ^2H substitution at the four meso-carbon positions (d_4) and pyrrole ^{15}N substitution. The isotope shifts are listed in Table I; they are quite similar for corresponding bands, both polarized and depolarized, of the parent NiOEP and its radical cation. Thus the ν_4 bands (1383 and 1368 cm^{-1}, p) are ^{15}N-sensitive (7 cm^{-1} for NiOEP and 10 cm^{-1} for $NiOEP^{\bullet+}$) but d_4-insensitive, while the reverse is true for the ν_3 (1519 and 1511 cm^{-1}, p) and ν_{10} (1653 and 1644 cm^{-1}, dp) bands. The ν_2/ν_{11} pair (1600/1575 and 1623/1608 cm^{-1}, p/dp) show neither d_4 nor ^{15}N sensitivity. The isotope shifts imply similar eigenvectors for the modes; on this basis we can confidently assign the radical cation bands to the same set of normal modes as in the neutral porphyrin, which have been analyzed in detail.[10] This result supports the analysis of $MOEP^{\bullet+}$ RR frequencies by Oertling et al., who found core-size dependencies for the high-frequency modes which parallel those of the neutral porphyrin counterparts.[5]

Likewise the metallo-TPP normal modes are essentially unchanged upon radical formation. Figure 4 compares 457.9-nm excited spectra of CuTPP and $CuTPP^{\bullet+}$ isotopomers with ^2H substituted at the pyrrole C_β (d_8) or the phenyl carbon atoms (d_{20}). The isotopic data are listed in Table II, where it is seen that the isotope shift patterns are very similar. The MTPP normal modes have likewise been analyzed in detail.[9]

3. Skeletal Mode Frequency Shifts Differ for OEP and TPP Radicals. In Table III the mode frequencies are listed for neutral and radical OEP complexes of Ni^{2+}, Cu^{2+}, VO^{2+}, and Fe^{3+} (chloride adduct). The pattern of frequency shifts upon radical formation is seen to be very similar for all four complexes. Large upshifts, 20–30 cm^{-1}, are found for ν_2 and ν_{11}. The ν_4 mode shifts down appreciably (12–15 cm^{-1}), while smaller downshifts, 2–9 cm^{-1}, are found for ν_{10} and ν_3. The remaining mode shifts are small, 0–4 cm^{-1}. A similar pattern was observed for several OEP cation radicals by Oertling et al.[8]

The TPP complexes also give rise to a consistent set of frequency shifts upon radical formation, as shown in Table IV, but the pattern is different from that of the OEP complexes. Figure 5 demonstrates these patterns graphically for the Cu^{2+} complexes of OEP and TPP. The major difference is that ν_2 and ν_{11} shift up on radical formation in OEP but down in TPP. The difference is particularly striking for ν_2 which is one of the strongest bands in both sets of spectra.

4. A_{2g} Modes Reflect Major Perturbations. In addition to the polarized and depolarized bands, the 406.7-nm excited RR spectrum of $NiOEP^{\bullet+}$ contains a pair of fairly prominent anomalously polarized bands, at 958 and 1166 cm^{-1}. These are dis-

Table IV. Resonance Raman Frequencies (cm^{-1}) for Metallotetraphenylporphyrins and Their Cation Radicals[a]

ρ	CuTPP	CuTPP$^{\bullet+}$	Δ	NiTPP	NiTPP$^{\bullet+}$	Δ	ClFeTPP	ClFeTPP$^{\bullet+}$	Δ	assignment[b]
p	1599	1595	−4	1599	1595	−4	1598	1596	−2	ν(phenyl)
dp	1582	1586	+4	1594				1589		ν_{10}, $\nu(C_\alpha-C_m)_{asym}$
p	1562	1530	−32	1570	1532	−38	1553	1526	−27	ν_2, $\nu(C_\beta-C_\beta)$
dp		1360		1377	1359	−18		1358		ν_{29}, ν(pyr. quarter ring)
p	1365	1355	−10	1374	1370	−4	1363	1345	−18	ν_4, $\nu(\text{pyr. half ring})_{sym}$
p	1237	1234	−3	1236	1234	−2	1233	1234	+1	ν_1, $\nu(C_m-Ph)$
dp	1185	1181	−4	1183	1181	−2		1183		$\delta(C_{Ph}-H)$
p	1080	1077	−3	1080			1081	1082	+1	$\delta(C_\beta-H)_{sym}$
ap		1044						1021		A_{2g} mode[c]
p	1008	1002	−6	1006	1003	−3	1005	1003	−2	ν(pyr. breathing)
ap		959								A_{2g} mode[c]
ap		899						902		A_{2g} mode[c]
p	886	884	−2	888	889	+1		888		$\delta(\text{pyr. def.})_{sym}$

[a] Observed frequencies from CH_2Cl_2/0.1 M TBAP solution spectra (457.9-nm excitation). Δ = frequency shifts (cm^{-1}) upon cation radical formation; p, dp, and ap = polarized, depolarized, and anomalously polarized bands, respectively. [b] See ref 9 for mode descriptions. [c] New bands seen only in radical cation spectra.

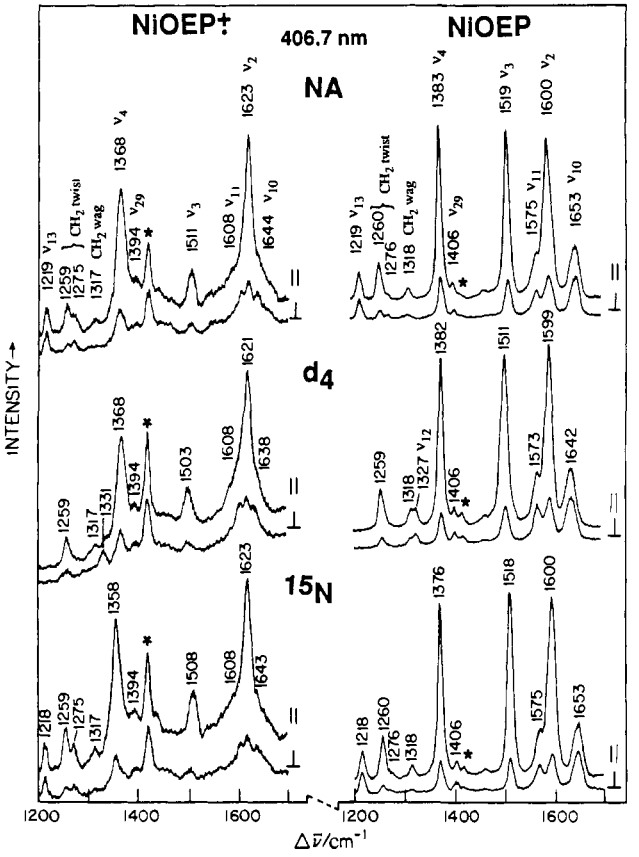

Figure 3. Resonance Raman spectra of NiOEP and NiOEP$^{\bullet+}$ and their ^{15}N and *meso*-d_4 isotopomers in parallel and perpendicular polarizations. Spectra were obtained with 406.7-nm excitation, 50-mW laser power, and 8-cm^{-1} slitwidths. Asterisks indicate CH_2Cl_2 solvent bands.

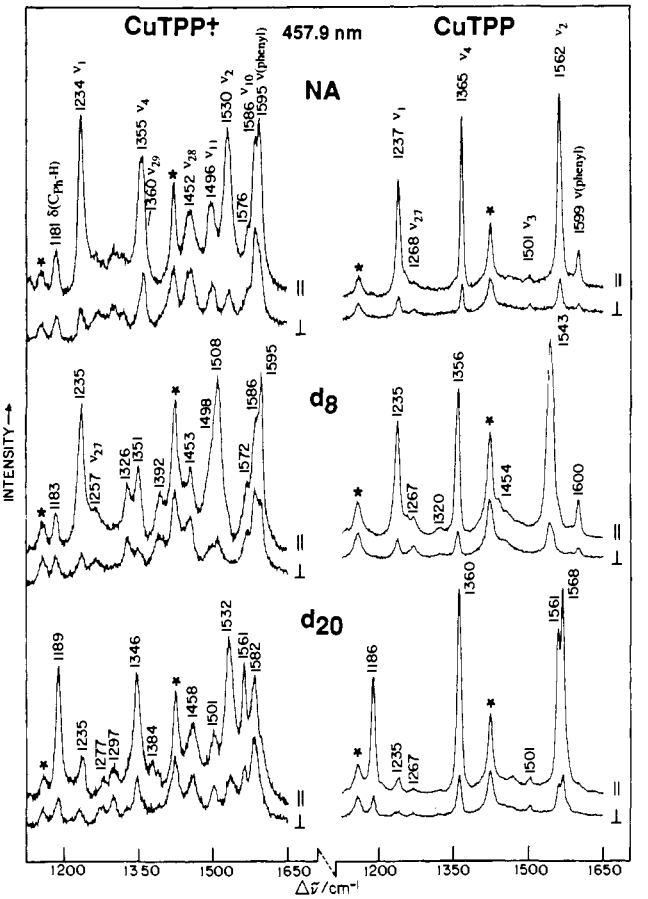

Figure 4. Resonance Raman spectra of CuTPP and CuTPP$^{\bullet+}$ and their pyrrole-d_8 and phenyl-d_{20} isotopomers in parallel and perpendicular polarizations. Spectra were obtained with 457.9-nm excitation, 50-mW laser power, and 8-cm^{-1} slitwidths. Asterisks indicate CH_2Cl_2 solvent bands.

cernible in Figure 1 and are seen more clearly in Figure 6 where the 900–1200-cm^{-1} region is isolated. Also shown in Figure 6 are the same regions of the Soret-excited RR spectra of radical cations of other OEP complexes, with Zn^{2+}, Cu^{2+}, and VO^{2+}. All of these contain the two ap bands, and their frequencies vary somewhat, showing a significant sensitivity to the metal. They are also sensitive to ^{15}N and/or d_4 substitution, as shown in Figure 7. The 958-cm^{-1}, but not the 1166-cm^{-1} band is significantly (7 cm^{-1}) sensitive to ^{15}N substitution.

The isotope shifts make it clear that these bands arise from molecular vibrations, and not from electronic Raman transitions. Both bands are strongly shifted upon meso-deuteration. The 9-cm^{-1} ^{15}N shift of the 908-cm^{-1} d_4 isotopomer band identifies it with the 958-cm^{-1} h_4 band, establishing a 50-cm^{-1} downshift. The 1166-cm^{-1} h_4 band appears to be replaced in the d_4 isotopomer with two bands at much lower frequency, 989 and 959 cm^{-1}. In D_{4h} symmetry, ap bands arise from modes classifying as A_{2g}. These modes have all been identified for NiOEP,[10,26] and are listed in Table V. It can be seen that the NiOEP$^{\bullet+}$ ap bands do not correspond, either in frequency or isotope shift pattern to any of the NiOEP ap modes.

We considered the possibility that the NiOEP$^{\bullet+}$ ap bands arise from vibrations other than A_{2g} modes. They must be in-plane modes of the porphyrin, since the out-of-plane modes are all below 850 cm^{-1} for OEP's.[26] If the molecular symmetry is lowered sufficiently, then non-A_{2g} modes can correlate with modes having antisymmetric scattering tensor elements. In particular, if the symmetry were lowered to C_{4v} or D_{2d}, as in the case of domed or

(26) Li, X-Y.; Czernuszewicz, R. S.; Kincaid, J. R.; Spiro, T. G. *J. Am. Chem. Soc.*, in press.

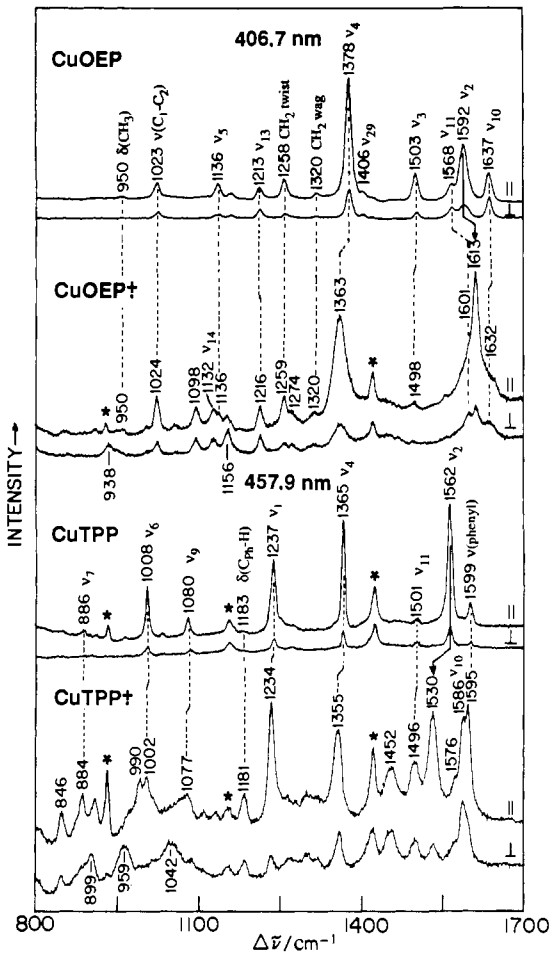

Figure 5. Comparison of the resonance Raman spectra of CuOEP/CuOEP$^{\bullet+}$ and CuTPP/CuTPP$^{\bullet+}$. Spectra were obtained with 406.7-nm (CuOEP and CuOEP$^{\bullet+}$) and 457.9-nm (CuTPP and CuTPP$^{\bullet+}$) excitation wavelengths, 50-mW laser power, and 8-cm^{-1} slitwidths. The ν_2 upshift for CuOEP$^{\bullet+}$ and downshift for CuTPP$^{\bullet+}$ are indicated with arrows. Asterisks indicate ClO_4^- (electrolyte) and CH_2Cl_2 solvent bands.

Table V. Resonance Raman Frequencies and ^{15}N Isotope Shifts (cm^{-1}) for A_{2g} Modes of NiOEP and NiOEP$^{\bullet+}$ and Their *meso*-d_4 Isotopomers

		NiOEP[a]		NiOEP$^{\bullet+}$[b]	
mode	Assignment	NA	*meso*-d_4	NA	*meso*-d_4
ν_{19}	$\nu(C_\alpha-C_m)_{asym}$	1603 (1)[c]	1581 (1)		
ν_{20}	ν(pyr. quarter ring)	1393 (1)	1393 (1)		
					1331 (1)[e]
ν_{21}	$\delta(C_m-H)$	1307 (4)	887 (4)		
				1166 (2)	959 (1)
ν_{22}	ν(pyr. half ring)$_{asym}$	1121 (14)	1202 (12)		
ν_{23}	$\nu(C_\beta-C_1)_{asym}$	1058 (1)	1058 (1)		
					989 (1)[e]
				958 (7)	908 (9)
ν_{24}	δ(pyr. def.)$_{asym}$	597 (1)	582 (1)		
ν_{25}	δ(pyr. rot.)	551 (1)	545 (0)		
ν_{26}	$\delta(C_\beta-C_1)_{asym}$	[243] [0][d]	[243] [0]		

[a] Observed values (CS_2 solution, 530.9-nm excitation) and assignments taken from ref 10. NA = natural abundance; *meso*-d_4 = ^2H substituted analogues at meso carbon positions. [b] This work; observed values from CD_2Cl_2/0.1 M TBAT solution spectra (406.7-nm excitation). [c] Numbers in parentheses indicate downshifts upon pyrrole-^{15}N substitution. [d] Calculated values in brackets.[26] [e] Seen only in *meso*-d_4 isotopomer spectra.

ruffled porphyrins, the E_u modes would become E, which can in principle have anomalous polarization (depending on the relative magnitude of symmetric and antisymmetric tensor elements).[27] However, the E modes have no effective resonance enhancement mechanism. Being nontotally symmetric they are not subject to Franck-Condon (A term) enhancement; they cannot vibronically couple (B term) the dominant in-plane electronic transitions, which are themselves of E symmetry, since $E \times E = A_1 + A_2 + B_1 + B_2$ does not contain the E representation. If the molecular symmetry were lowered further, the E modes would split into A and B components; the latter might be anomalously polarized and might even be vibronically active. But this would require loss of the *x*,*y* equivalency in the porphyrin plane. There is no plausible physical mechanism for *x*,*y* inequivalency in a 4-fold symmetric porphyrin or its radical cation. Even if these qualitative arguments against a non-A_{2g} origin for the ap bands could be overcome, we have been unable to find any modes, among any of the NiOEP in-plane vibrations,[10] which correspond at all closely with the frequencies and isotope shifts for the NiOEP$^{\bullet+}$ ap bands.

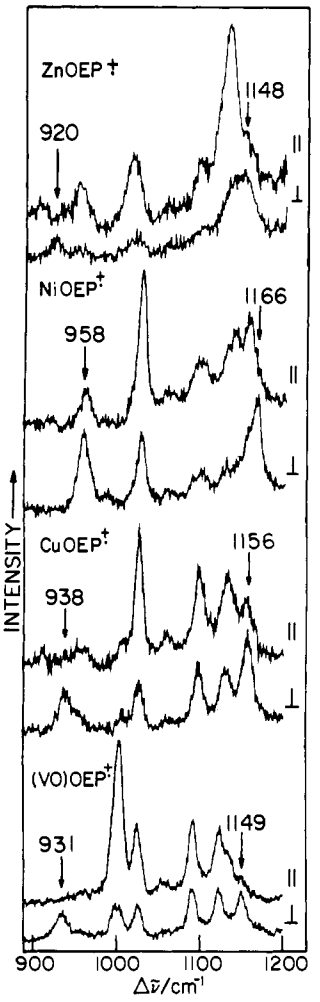

Figure 6. Anomalously polarized bands in the Soret excited resonance Raman spectra of ZnOEP$^{\bullet+}$, NiOEP$^{\bullet+}$, CuOEP$^{\bullet+}$, and OVOEP$^{\bullet+}$. Spectra were obtained with 30–50-mW laser power and 8-cm^{-1} slitwidths using 406.7-nm (Ni, Cu, VO) and 363.8-nm (Zn) excitation wavelengths.

We therefore conclude that these bands *do* arise from A_{2g} modes, but that their frequencies and normal mode compositions are quite different from those of the parent NiOEP. Two of the latter show strong d_4 effects (Table V): the 1307- and 1121-cm^{-1} modes, ν_{21} and ν_{22}, are replaced by bands at 887 and 1202 cm^{-1} in the d_4 isotopomer of NiOEP, reflecting heavy involvement of the δC_mH bending coordinate. Since the two NiOEP$^{\bullet+}$ ap bands at 1166 and 958 cm^{-1} are also strongly shifted in the d_4 isotopomer, we conclude that these two A_{2g} mode frequencies are at least 150 cm^{-1} lower than corresponding modes in NiOEP. That the d_4 (and ^{15}N) shifts are quantitatively dissimilar for the NiOEP and NiOEP$^{\bullet+}$ ap bands can be attributed to normal mode remixing due to the large frequency changes. Because this remixing makes the mode correspondences unrecognizable, the ~150-cm^{-1} frequency lowering estimate must be considered a lower limit. Since most of the A_{2g} modes have not been detected in NiOEP$^{\bullet+}$, we cannot estimate the force constant changes that are involved.

(27) McClain, W. M. *J. Chem. Phys.* **1971**, *55*, 2789–2796.

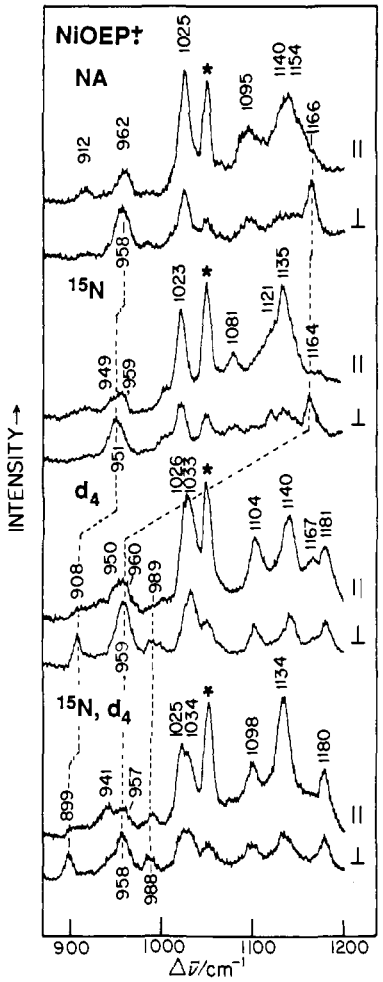

Figure 7. ^{15}N and *meso*-d_4 isotope sensitivity for the anomalously polarized bands of $NiOEP^{+}$. These spectra were obtained with 406.7-nm excitation (50 mW) and 8-cm^{-1} slitwidths. The dashed lines correlate the ap bands. Asterisks indicate CD_2Cl_2 solvent bands.

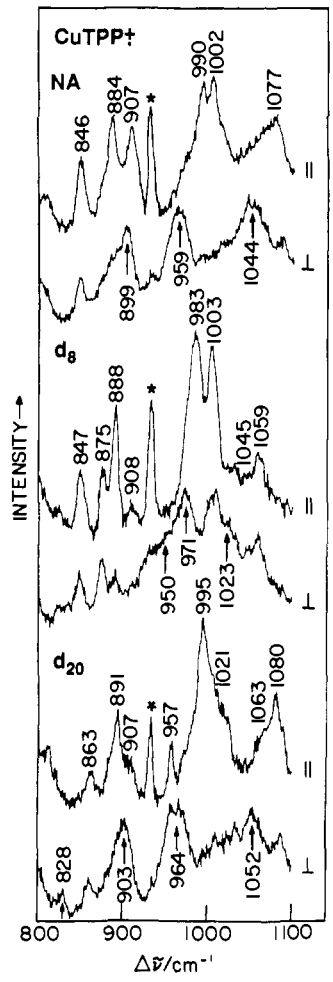

Figure 8. Isotope sensitivity upon ^{2}H substitution in the pyrrole C_β and phenyl carbon (d_{20}) positions for the anomalously polarized bands of $CuTPP^{+}$; all spectra were obtained with 457.9-nm excitation (50 mW) and 8-cm^{-1} slitwidths. Arrows indicate the positions of the anomalously polarized bands. Asterisks indicate CH_2Cl_2 solvent bands.

There can be little doubt, however, that radical formation introduces a major perturbation of the A_{2g} modes, whereas the A_{1g} and B_{1g} modes suffer only minor alterations.

Figure 8 shows a similar effect for $CuTPP^{+}$. The 457.9-nm excited RR spectrum contains three bands, at 1044, 959, and 899 cm^{-1}, with significant anomalous polarization. They are all affected by deuteration at the pyrrole or phenyl positions, or both; the d_{20} spectrum actually shows four ap bands. The A_{2g} modes have been analyzed for NiTPP,[9] but not CuTPP. The substitution of Cu for Ni is expected to produce some frequency differences, but the isotope shift pattern should be unaltered. The $CuTPP^{+}$ ap bands lack any correspondence with the NiTPP A_{2g} modes.[9]

Discussion

1. Cation Radical A_{2g} Modes Are Pseudo-Jahn–Teller Active. Porphyrins have two closely spaced highest occupied molecular orbitals (HOMOs), of a_{1u} and a_{2u} symmetry in the idealized D_{4h} point group.[4] Removal of an electron leads to a radical with an A_{1u} or A_{2u} ground state, depending on which orbital lies higher in energy. Because of the small energy gap, there is also a low-lying excited state, of A_{2u} or A_{1u} symmetry, respectively. The ground and excited states are subject to vibronic coupling; their near-degeneracy can be expected to produce a pseudo-Jahn–Teller (pJT) effect.[28] The symmetry of the modes capable of pJT mixing is given by the cross product $A_{1u} \times A_{2u} = A_{2g}$. The consequences of this mixing are that the two mixed states have a larger energy separation, so that the ground state is stabilized, and the mixing modes are lowered in vibrational frequency. This mechanism provides a natural explanation of the greatly lowered ap band frequencies of the radical cations, discussed in the preceding section. The pJT effect is illustrated in Figure 9. As a function of a mixing coordinate, Q_k, the energy of the states is given by

$$E_{\pm} = \tfrac{1}{2}F_{kk}Q_k^2 \pm (\Delta^2 + f_k^2Q_k^2)^{1/2} \qquad (1)$$

where F_{kk} is the harmonic force constant,

$$\left\langle \psi_i \left| \left(\frac{\partial^2 V}{\partial Q^2{}_k} \right)_{Q_0} \right| \psi_i \right\rangle \qquad (i \text{ is } A_{1u} \text{ or } A_{2u})$$

while f_k is the linear vibronic coupling constant,

$$\left\langle \psi_i \left| \left(\frac{\partial V}{\partial Q_k} \right)_{Q_0} \right| \psi j \right\rangle \qquad (i \neq j\ (A_{1u}, A_{2u}))$$

and Δ is half the A_{1u}–A_{2u} energy separation in the absence of mixing. The effect of the linear vibronic term is to flatten the ground-state potential curve, thereby lowering the mode frequency. If the mixing is strong enough (large f_k and small Δ), a double minimum potential results and the molecule distorts along the mixing coordinate. Since the A_{2g} modes have the symmetry of a molecular rotation, the resulting distortion would involve parts of the ring rotating against one another, i.e., alternation of the $C_\alpha C_m$, NC_α, or $C_\alpha C_\beta$ bond lengths, or bending of all the C_m–X or all the C_β–Y substituent bonds in the same direction. Most of the available radical cation X-ray crystal structures[16-21] show no clear evidence for this kind of distortion. However, a very recent

(28) (a) Engleman, R. *The Jahn–Teller Effect in Molecules and Crystals*; Wiley-Interscience: New York, 1972. (b) Siebrand, W.; Zgierski, M. In *Excited States*; Lim, E. C., Ed.; Academic Press: New York, 1979; Vol. 4, pp 1–136.

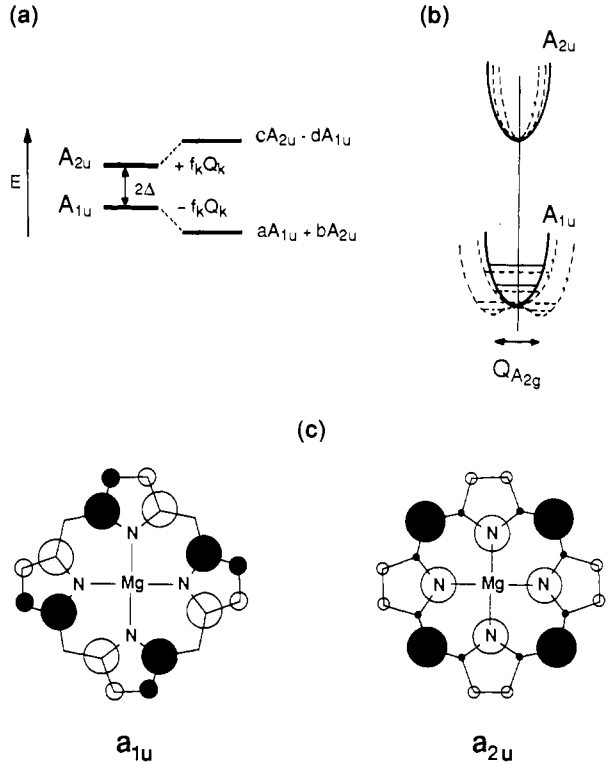

Figure 9. Illustration of the pJT effect. (a) Energy levels of the unperturbed ground (A_{1u}) and excited (A_{2u}) states and of the final states mixed by linear vibronic coupling. (b) Potential curves for the unperturbed (solid lines) and mixed (dashed lines) states along an A_{2g} mixing coordinate. Depending on the degree of mixing, the lower curve is broadened or converted to a double minimum potential. (c) The atomic orbital (AO) structure of magnesium porphine in the two highest occupied molecular orbitals, a_{1u} and a_{2u}. The circle sizes are approximately proportional to the AO coefficients: 0.3055 (C_α) and 0.1600 (C_β) for the a_{1u} orbital, and 0.0190 (C_α), 0.0728 (C_β), 0.4101 (C_m), and 0.2645 (N) for the a_{2u} orbital. The open circles represent negative signs of the upper lobe of the p_π AO's (from ref 33).

crystal structure of $MgOEP^{\bullet+}$ by Scheidt and co-workers[21b] shows the effect very nicely. This structure reveals a definite bond alteration around the 16-membered inner ring, leading to effective C_4 symmetry. The inequivalent bonds differ by ~0.04 Å.

If this distortion were to persist in solution, then the anomalous polarization of the pJT modes might be difficult to detect since A_{2g} correlates with A in the C_4 point group. Since large $I_\perp/I_\parallel$ ratios are seen in the spectra (Figure 6), we infer that the pJT distortion is dynamic in character and is frozen out by the lattice forces in the $MgOEP^{\bullet+}$ crystals.

2. Does the pJT Effect Result in a Saddle Distortion? A notable feature of the available radical cation crystal structures is the occurrence of a saddle distortion, in which opposite pyrrole rings are alternately displaced up and down relative to the mean porphyrin plane. Figure 10 shows this distortion for $(Cl^-)Fe^{III}TPP^{\bullet+}$;[18,20] the neutral species has a nearly flat porphyrin ring. A saddle distortion is also seen for $MgTPP^{\bullet+}$,[19] $ZnTPP^{\bullet+}$,[16] and $CuTPP^{\bullet}$,[17] but not for $(ClO_4^-)_2Fe^{III}TPP^{\bullet+}$.[20]

The saddle distortion corresponds to displacement of the porphyrin along a B_{2u} out-of-plane coordinate. Also shown in Figure 10 are the two lowest frequency B_{2u} pyrrole translational modes, γ_{17} and γ_{18}, calculated for NiOEP at 127 and 30 cm^{-1}, respectively;[26] a marked resemblance to the observed saddle distortion can be seen. B_{2u} modes are not vibronically active in D_{4h} symmetry. But if the symmetry is lowered to D_{2d}, then the B_{2u} modes are transformed to A_2, as are the A_{2g} modes, and they can mix the A_{1u} and A_{2u} (now B_1 and B_2) states. The saddle distortion itself leads to D_{2d} symmetry. Consequently, the potential minimum along the low-energy B_{2u} coordinates may be displaced from the planar structure due to the effects of pJT mixing. Thus there is an electronic reason for expecting a saddle distortion.

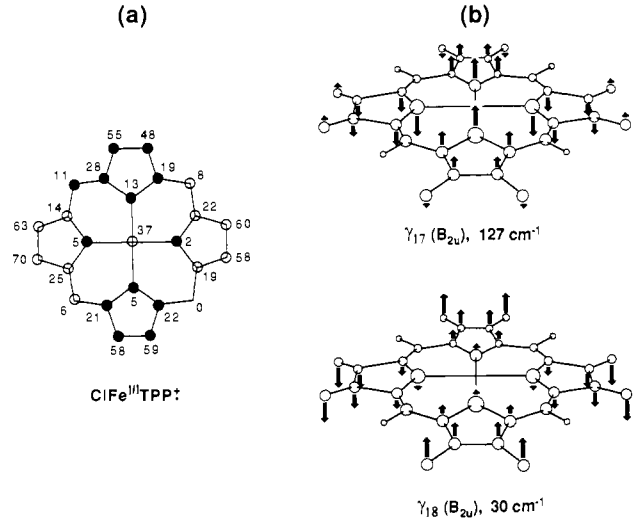

Figure 10. Illustration of the similarity between the atom displacements (0.01 Å units) for $ClFe(III)TPP^{\bullet+}$ determined by X-ray crystallography[30] (a) and the B_{2u} (D_{4h} symmetry) out-of-plane vibrational modes of NiOEP calculated[26] at 30 cm^{-1} (γ_{18}) and 127 cm^{-1} (γ_{17}). γ_{17} is observed at this frequency in the tetragonal crystalline form of NiOEP[26] (b).

Other factors may also contribute, however. Crystal-packing effects are certainly important,[29] and Scheidt has pointed out[30] that the saddle distortion permits more extensive intermolecular interactions between radicals in the crystal than a planar porphyrin would. The fact that a saddle distortion is not seen for $(ClO_4^-)_2Fe^{III}TPP^{\bullet+}$,[20] in contrast to $(Cl^-)Fe^{III}TPP^{\bullet+}$,[18,20] indicates that if there is a pJT-induced saddle distortion it is weak enough to be suppressed by the (presumably steric) effects of a change from five- to six-coordination. A saddle distortion is not seen for $MgOEP^{\bullet+}$.[21b]

Unfortunately, we do not know whether a saddle distortion is present for radical cations in solution. Low-frequency RR bands which might be diagnostic for such a distortion are being sought, but have not so far been detected. Oertling et al.[8] have argued that out-of-plane distortions are unlikely in view of the good correlations of the high-frequency $MOEP^{\bullet+}$ modes with the (expected) porphyrin core size. They cited the significant frequency shifts seen for the ruffled vs the planar form of NiOEP[26,31] as representative of the deviations that might be expected if the $MOEP^{\bullet+}$ radicals were nonplanar. This argument is not conclusive, however, because the core size correlations would be maintained if all the $MOEP^{\bullet+}$s were subject to similar distortion and induced frequency shifts, or if the shifts were themselves correlated with core size. Thus the issue of intrinsic radical structure, free of intermolecular influences, cannot presently be resolved.

3. TPP and OEP Radicals Are Predominantly A_{2u} and A_{1u}. The LCAO coefficients of the a_{1u} and a_{2u} molecular orbitals are diagrammed in Figure 9. The size of the circles are proportional to the coefficients of the atomic p_z orbitals and the shading refers to their signs on one side of the ring. We note that while these patterns, originally developed by Longuet-Higgins[32] from semiempirical LCAO calculations, have many times been reproduced, the a_{2u} orbital is generally shown as having zero coefficients at the pyrrole C_β atoms. It has been shown, however, that calculations at the more accurate ab initio SCF-MO level lead to appreciable coefficients at the C_β atoms.[15,33] The circles in Figure 9 are based on the ab initio orbital coefficients.[33] The expectation

(29) Hoard, J. L. In *Porphyrins and Metalloporphyrins*; Smith, K. M., Ed.; Elsevier: New York, 1975; pp 317–376.
(30) Scheidt, W. R.; Lee, Y. J. *Struct. Bonding* **1987**, *64*, 1–70.
(31) Spaulding, L. D.; Chang, C. C.; Yu, N. T.; Felton, R. H. *J. Am. Chem. Soc.* **1975**, *97*, 2517–2525.
(32) Longuet-Higgins, H. C.; Rector, C. W.; Platt, J. R. *J. Chem. Phys.* **1950**, *18*, 1174–1181.
(33) Spangler, D.; Maggiora, G. M.; Shipman, L. L.; Christofferson, R. E. *J. Am. Chem. Soc.* **1977**, *99*, 7478–7489. The orbital coefficients shown in Figure 9 were kindly supplied by Dr. James Petke.

is that the a_{2u} orbital has a bonding interaction between C_β atoms of a given pyrrole ring, while the a_{1u} interaction is antibonding. This is a key point in the interpretation of the RR frequency shifts upon radical formation, as discussed below.

The squares of the atomic orbital coefficients should be proportional to the spin densities on the radical cations. Thus, a radical with purely a_{1u} character should have zero spin densities at the C_m and N atoms. In fact, EPR measurements[14] and ab initio calculations[15] show that these positions are not devoid of spin density, indicating that the a_{1u} and a_{2u} states are mixed as a general rule. The pJT effect, discussed in the preceding section, provides a general mechanism for this mixing. Nevertheless, the radicals can have predominantly a_{1u} or a_{2u} character, depending on the energy separation of the unmixed orbitals and the magnitude of the pJT effect. Thus the MTPP radicals so far examined by magnetic resonance techniques show much greater spin density on the C_m than on the C_α or C_β atoms, consistent with mainly a_{2u} character.[12]

The situation with respect to the MOEP radicals is less clear-cut. Detailed EPR studies have shown $MgOEP^{\bullet+}$ and $ZnOEP^{\bullet+}$ to be mainly a_{1u} in character.[12] For other MOEP radicals, optical spectra which differ from those of $MgOEP^{\bullet+}$ and $ZnOEP^{\bullet+}$ have been attributed to a_{2u} character;[13] often EPR data are unavailable or uninterpretable in these cases because of magnetic interactions. In a celebrated study the radical character of $Co^{III}OEP^{\bullet+}$ was reported to depend on the axial ligand.[34] On the basis of the optical spectra, a_{2u} and a_{1u} character were assigned respectively to the ClO_4^- and Br^- adducts. The two kinds of optical spectra have been rationalized on the basis of INDO/S-CI calculations by Edwards and Zerner.[35] Yet the Co hyperfine coupling constant has been reported to be only 1.2 G for $(ClO_4^-)_2Co^{III}OEP^{\bullet+}$, compared with 5.6–5.7 G for the $(ClO_4^-)_2Co^{III}TPP^{\bullet+}$ species.[36] A large hyperfine constant is expected for an a_{2u} radical because of the concentration of spin density on the pyrrole N atoms which can delocalize onto the metal. The much smaller value observed for $(ClO_4^-)_2Co^{III}OEP^{\bullet+}$ suggests mainly a_{1u} character, contrary to the optical assignment. Also a recent NMR study[37] suggests a_{1u} character for $CuOEP^{\bullet+}$, whose optical spectrum[13] resembles $(ClO_4^-)_2Co^{III}OEP^{\bullet+}$ more than $(Br^-)_2Co^{III}OEP^{\bullet}$; the C_mH proton shows a downfield shift, whereas an upfield shift is expected for an a_{2u} radical because of the spin density on C_m. These magnetic resonance results indicate that the optical spectrum is not a reliable indicator of radical type.

This conclusion was anticipated some time ago by Gouterman and co-workers,[4b] whose analysis of metalloporphyrin spectra led to the expectation that MOEP cation radicals should all be a_{1u} in character. This expectation is fully supported by the $MOEP^{\bullet+}$ RR bands. When their frequencies are compared with those of the neutral species (Table II), the most striking changes are the upshifts in ν_2 and ν_{11}, $\sim$22 and $\sim$33 cm^{-1}, respectively, and the downshift in ν_4, $\sim$14 cm^{-1}. Similar up- and downshifts of ν_2 and ν_4 have been observed for $ZnOEP^{\bullet+}$, $(ClO_4^-)_2CoOEP^{\bullet+}$, and $(Br^-)_2CoOEP^{\bullet+}$ by Oertling et al.[8] (The report by Kim et al.[6] of opposite shifts for $ZnOEP^{\bullet+}$, $MgOEP^{\bullet+}$, and $(Br^-)_2CoOEP^{\bullet+}$ was due to contamination by H_4OEP^{2+}, as noted in the Introduction.) This shift pattern is in accord with expectation for radicals with predominant a_{1u}, but not a_{2u} character. The ν_2 and ν_{11} modes involve $C_\beta C_\beta$ stretching, mainly, and their upshifts are consistent with the antibonding character of the a_{1u} orbital with respect to the $C_\beta C_\beta$ bonds. Removal of an electron is expected to increase the $C_\beta C_\beta$ bond strength and raise the stretching frequency. The a_{2u} orbital, however, is bonding with respect to the $C_\beta C_\beta$ bonds. Removal of an electron should weaken the bonds and decrease the stretching frequency. This is exactly what is seen for the TPP complexes; ν_2 shifts down by $\sim$30 cm^{-1} for $CuTPP^{\bullet+}$, $NiTPP^{\bullet+}$, and $(Cl^-)FeTPP^{\bullet+}$ relative to the neutral species (Table IV). The assignment of ν_2 to a mode involving predominant $C_\beta C_\beta$ stretching in both kinds of porphyrins is secured by the isotope shifts (Tables I and II) and by recent normal coordinate calculations.[9,10] There is also some contribution of $C_\alpha C_m$ stretching to ν_2, particularly for TPP complexes.[9] The a_{2u} orbital is also bonding with respect to the $C_\alpha C_m$ bonds, and electron removal should also decrease the $C_\alpha C_m$ bond strength.

The ν_4 mode has been considered[24] to be $C_\alpha N$ stretching in character, but the recent normal mode analyses[9,10] establish that a more apt description is the pyrrole symmetric half-ring stretch, in which the $C_\alpha N$ and $C_\alpha C_\beta$ bonds stretch out-of-phase. The a_{1u} orbital is nonbonding with respect to the $C_\alpha N$ bonds (node at N) but bonding with respect to the $C_\alpha C_\beta$ bonds. Thus, the downshift of ν_4 which is seen consistently for the OEP complexes is as expected for predominant a_{1u} character. In the a_{2u} orbital both the $C_\alpha N$ and $C_\alpha C_\beta$ interactions are nearly nonbonding, and the ν_4 shifts are smaller and variable.

In summary, these frequency shift patterns are consistent with predominant a_{2u} character for all the TPP radicals and predominant a_{1u} character for all the OEP radicals. Oertling et al.,[8] noting the similar shifts for all OEP radicals despite their previous differentiation based on optical spectra, suggested that the frequency shifts are independent of radical type. The shifts seen for TPP radicals, however, contradict this inference. In view of the equivocal character of the classification based on optical spectra, with magnetic resonance counter-indications as discussed above, the RR evidence for common a_{1u} character for the OEP radicals is persuasive.

Moreover, a simple electronic explanation can be offered for the orbital selectivities of TPP and OEP based on the substituent pattern. The phenyl groups at the meso positions of TPP should raise the energy of the a_{2u} relative to the a_{1u} orbital via the interaction of the filled phenyl and porphyrin π orbitals, since electron density is concentrated at the C_m atoms for the a_{2u} orbital, while the a_{1u} orbital has a node at C_m. In the case of OEP, the ethyl groups should donate some electron density to the C_β atoms. Both orbitals have electron density at the C_β atoms but the C_β coefficients are slightly larger for the a_{1u} orbital, suggesting that it is destabilized more by interactions with the filled ethyl orbitals. Thus the position of the substituents alone suggests that electron removal would leave a hole in the a_{2u} orbital for TPP's but in the a_{1u} orbital for OEP's, consistent with the experimental results.

An important caveat, however, is that these arguments apply to metalloporphyrins with no, or only weak, axial ligands. Fajer and co-workers have shown, via extended Hückel calculations, that the a_{1u} orbital is increasingly stabilized, relative to the a_{2u} orbital with increasing donor strength of the axial ligand(s).[38] This trend can also be understood qualitatively from simple electronic arguments. The a_{2u} orbital concentrates electron density on the pyrrole N atoms, while the a_{1u} orbital has nodes at these positions. Thus the electropositive metal ion stabilizes the a_{2u} orbital more than the a_{1u} orbital, but this tendency is countered by electron donation from the ligand. Increasingly strong donor ligands destabilize the a_{2u} orbital via this polarization effect, and possibly also by direct interaction of filled ligand π orbitals, when available (e.g., imidazole, thiolate) with the a_{2u} orbital. It is known that the horseradish peroxidase (HRP) compound I intermediate contains a ferryl porphyrin cation radical, which has predominant a_{2u} character.[39] Since the porphyrin in HRP is protoporphyrin IX, with the same substituent pattern as OEP, we would expect the radical to have predominant a_{1u} character, but the donor effects of the oxo ligand on one side, and a proximal histidine ligand on the other, are evidently sufficient to reverse the normal ordering and tip the balance in favor of a_{2u} character. We note that there have been several reports of HRP compound I RR spectra,[40-42]

(34) Dolphin, D.; Forman, A.; Borg, D. C.; Fajer, J.; Felton, R. H. *Proc. Natl. Acad. Sci. U.S.A.* **1971**, *68*, 614–618.
(35) Edwards, W. D.; Zerner, M. C. *Can. J. Chem.* **1985**, *63*, 1763–1772.
(36) Wolberg, A.; Manassen, J. *J. Am. Chem. Soc.* **1970**, *92*, 2982–2991.
(37) Godziela, G. M.; Goff, H. M. *J. Am. Chem. Soc.* **1986**, *108*, 2237–2243.
(38) Hanson, L. K.; Chang, C. K.; Davis, M. S.; Fajer, J. *J. Am. Chem. Soc.* **1981**, *103*, 663–670.
(39) (a) Roberts, J. E.; Hoffman, B. M.; Rutter, R.; Hager, L. P. *J. Biol. Chem.* **1981**, *256*, 2118–2121. (b) Hanson, L. K.; Chang, C. K.; Davis, M. S.; Fajer, J. *J. Am. Chem. Soc.* **1981**, *103*, 663–670.
(40) Oertling, W. A.; Babcock, G. T. *J. Am. Chem. Soc.* **1985**, *107*, 6406–6407.

which are, however, in substantial disagreement. The most recent one, by Kincaid and co-workers,[42] does appear to show a downshifted ν_2, as we would expect for an a_{2u} radical.

We note that the a_{1u}–a_{2u} orbital energy separation should greatly influence the extent of vibronic mixing via the pJT effect. Thus the A_{2g} mode perturbation should vary with the nature of the substituents, the central metal, and the axial ligand. There is appreciable variation (18–40 cm^{-1}) among the ap band frequencies for the $OEP^{\bullet+}$ radicals examined in this study. The extent of perturbation is difficult to evaluate, however, since we do not know which modes of the neutral porphyrin are being perturbed. In some cases, $(Cl^-)FeOEP^{\bullet+}$ and $NiTPP^{\bullet+}$, no ap bands were observed. It is not clear whether this negative evidence reflects substantially altered mode mixing, resulting in weak enhancement or hiding of the bands in another spectral region, or simply ineffective resonance conditions at the available laser wavelengths.

4. Mechanisms of Resonance Enhancement. The radical cation RR spectra are strikingly different from those of neutral porphyrins in three respects. (1) For the OEP radicals, long-wavelength excitation enhances the same polarized bands as does short-wavelength excitation, while for the neutrals, dp and ap bands dominate the spectra excited in the long-wavelength Q bands. (2) For the radicals, in contrast to the neutrals, ap bands are enhanced with short-wavelength excitation. (3) Only two or three radical ap bands are seen, whereas in the neutrals most of the A_{2g} modes can be detected with Q-band excitation.

The first of these differences can be understood on the basis of Gouterman's four-orbital model.[4a] The orbital excitations from the a_{1u} and a_{2u} HOMOs to the e_g^* LUMOs are of the same symmetry (E_u), and because of the near-degeneracy they interact strongly, producing a substantial energy separation between the first two π–π^* states, Q and B. The orbital transition dipoles add up for the higher energy B transition and nearly cancel for the Q transition. Excitation in the B absorption band produces strong RR enhancement of totally symmetric modes, via the dominant A term scattering mechanism,[23,44] but this mechanism is much less effective for excitation in the Q band because it depends on the square of the transition moment. Instead the Q-resonant RR spectra of MP's show strong enhancement via the B-term mechanism[23,44] of nontotally symmetric modes which are effective in mixing the Q and B states vibronically. The B term depends on the product of the transition moment and its derivative with respect to the normal coordinate; this derivative is large when there is strong vibronic mixing.

These considerations are modified in the case of $MP^{\bullet+}$ because the different electron occupancies of the a_{1u} and a_{2u} orbitals reduce the extent of transition dipole cancellation in the Q band. In the simplest one-electron approximation, the B and Q transition moments are $\sim(2\mu_{a_{1u}} + 2\mu_{a_{2u}})$ and $\sim(2\mu_{a_{1u}} - 2\mu_{a_{2u}}) \sim 0$ for MP, but $\sim(\mu_{a_{1u}} + 2\mu_{a_{2u}})$ and $\sim(2\mu_{a_{2u}} - \mu_{a_{1u}}) \neq 0$ for $MP^{\bullet+}$. Consequently the A-term scattering strength should diminish in B-band resonance but increase in Q-band resonance for $MP^{\bullet+}$ relative to MP. It is also likely, as suggested by Oertling et al.,[8] that Q/B vibronic coupling is weaker for $MP^{\bullet+}$ than MP; this would be a natural consequence of the increased allowedness of the Q transition. Both effects would lead to the observed dominance of polarized bands in both Q- and B-resonant RR spectra of $MP^{\bullet+}$.

In addition, the hole in the $MP^{\bullet+}$ HOMO permits additional excitations from lower lying π orbitals, which are in the same energy region as the a_{1u}, $a_{2u} \rightarrow e_g^*$ excitations.[35] The new excited states complicate the optical spectrum, no doubt accounting for the broad $MP^{\bullet+}$ absorption bands (Figure 2). They may also contribute to the observed RR enhancements.

With regard to A_{2g} mode enhancements seen for the $MP^{\bullet+}$ radicals with short-wavelength excitation, the likeliest mechanism is the C term of Albrecht.[43] This is another term in the Taylor expansion of the Raman polarizability, but it involves vibronic coupling of the ground state with a low-lying excited state, instead of coupling between the resonant state and another excited state. (There is an unfortunate nomenclature confusion with the C term of Ziegler and Hudson,[44] which is still another term in the expansion, involving the square of the dipole moment derivative, which can produce overtone enhancement in resonance with forbidden transitions.)

The Albrecht C term is generally ignored because excited-state mixing into the ground state is usually unimportant, owing to the absence of low-lying excited states, but in the $MP^{\bullet+}$ radicals this mixing is important, as discussed above. The C term is expected to enhance the modes which produce the mixing, i.e., the A_{2g} modes which mix the A_{1u} and A_{2u} states. We can readily understand why the set of A_{2g} modes seen for $MP^{\bullet+}$ might not be the same as for MP because the requirements for Q–B mixing via the B term (in MP) need not be the same as for A_{1u}–A_{2u} mixing via the C term (in $MP^{\bullet+}$). Maximal enhancement at short wavelengths is expected for the $MP^{\bullet+}$ ap bands since the transition dipoles from both the ground and the low-lying excited states (A_{1u} and A_{2u}), which are larger for the B than the Q transitions, are prefactors for the C term.[43] Thus the appearance in the Soret-excited $MP^{\bullet+}$ spectra of a small number of drastically shifted A_{2g} modes can be explained by the pJT effect in combination with C-term enhancement.

On the other hand, the possibility must be considered that B-term enhancement of the A_{2g} modes is also important, especially as the new $MP^{\bullet+}$ transitions from the lower orbitals introduce new possibilities for vibronic coupling. We note in this connection that the $CuTPP^{\bullet+}$ ap bands were observed with 457.9-nm excitation; with 406.7-nm excitation directly in the Soret band, the ap bands were not seen. Thus an important role for an extra transition is suggested.

Conclusions

The RR spectra of metalloporphyrin radical cations reveal new anomalously polarized deuteration-sensitive bands which are attributed to A_{2g} modes whose frequencies are strongly depressed via vibronic mixing of the close-lying a_{1u} and a_{2u} states. Additionally, the saddle distortion observed in radical cation crystal structures is suggested to be a manifestation of a_{1u}/a_{2u} mixing, this time via a B_{2u} out-of-plane mode which becomes vibronically active (A_2) in the lowered symmetry (D_{2d}).

The remaining modes are readily correlated with the corresponding modes of the neutral porphyrins via their isotope shifts, which show the mode compositions to be essentially unaltered. The frequency shifts are suggested to be diagnostic of the predominant orbital character, a_{1u} or a_{2u}, of the radical ground state. In particular, the ν_2 mode, which is mainly $C_\beta C_\beta$ stretching in character, shifts up and down for a_{1u} and a_{2u} radicals, respectively, consistent with straightforward orbital symmetry considerations. The data indicate that TPP radicals are a_{2u} in character, as expected, and that all OEP radicals, not just those of Zn and Mg, are a_{1u}, at least in the absence of strong donor ligands. Absorption spectral indications to the contrary for $NiOEP^{\bullet+}$ and $CuOEP^{\bullet+}$ are believed to be unreliable.

Acknowledgment. We thank Drs. Martin Gouterman, Jack Fajer, Robert Scheidt, and James Petke for helpful discussions. This work was supported by Grants DE-ACO2-81-ER-10861 from the U.S. Department of Energy (T.G.S.) and DK35153 from the National Institutes of Health (to J.R.K.).

Note Added in Proof. Babcock and co-workers[45] have independently concluded that all $MOEP^{\bullet+}$ radicals are a_{1u} in character, based on further analysis of their RR spectra.

(41) Ogura, T.; Kitagawa, T. *J. Am. Chem. Soc.* **1987**, *109*, 2177–2179.
(42) Paeng, K. J.; Kincaid, J. R. *J. Am. Chem. Soc.* **1988**, *110*, 7913–7915.
(43) Tang, J.; Albrecht, A. C. In *Raman Spectroscopy - Theory and Practice*; Symanski, H. A., Ed.; Plenum Press: New York, 1970; Chapter 2.
(44) Ziegler, L. D.; Hudson, B. *J. Chem. Phys.* **1981**, *74*, 982–992.
(45) Oertling, W. A.; Salehi, A.; Chang, C. K.; Babcock, G. T. *J. Phys. Chem.* **1989**, *93*, 1311–1319.